Supporting Information

Carbon/Two-Dimensional $MoTe_2$ Core/Shell-Structured Microspheres as Anode Material for Na-Ion Batteries

Jung Sang Cho[1,2], *Hyeon Seok Ju*[1], *Jung-Kul Lee*[3,*], *Yun Chan Kang*[1,*]

[1]Department of Materials Science and Engineering, Korea University, Anam-Dong, Seongbuk-Gu, Seoul 136-713, Republic of Korea, E-mail: yckang@korea.ac.kr
[2]Department of Engineering Chemistry, Chungbuk National University, Chungbuk 361-763, Republic of Korea.
[3]Department of Chemical Engineering, Konkuk University, 1 Hwayang-dong, Gwangjin-gu, Seoul 143-701, Republic of Korea, E-mail: jkrhee@konkuk.ac.kr

Keywords: Molybdenum telluride; Sodium ion batteries; Anode materials; Carbon composite; Spray pyrolysis

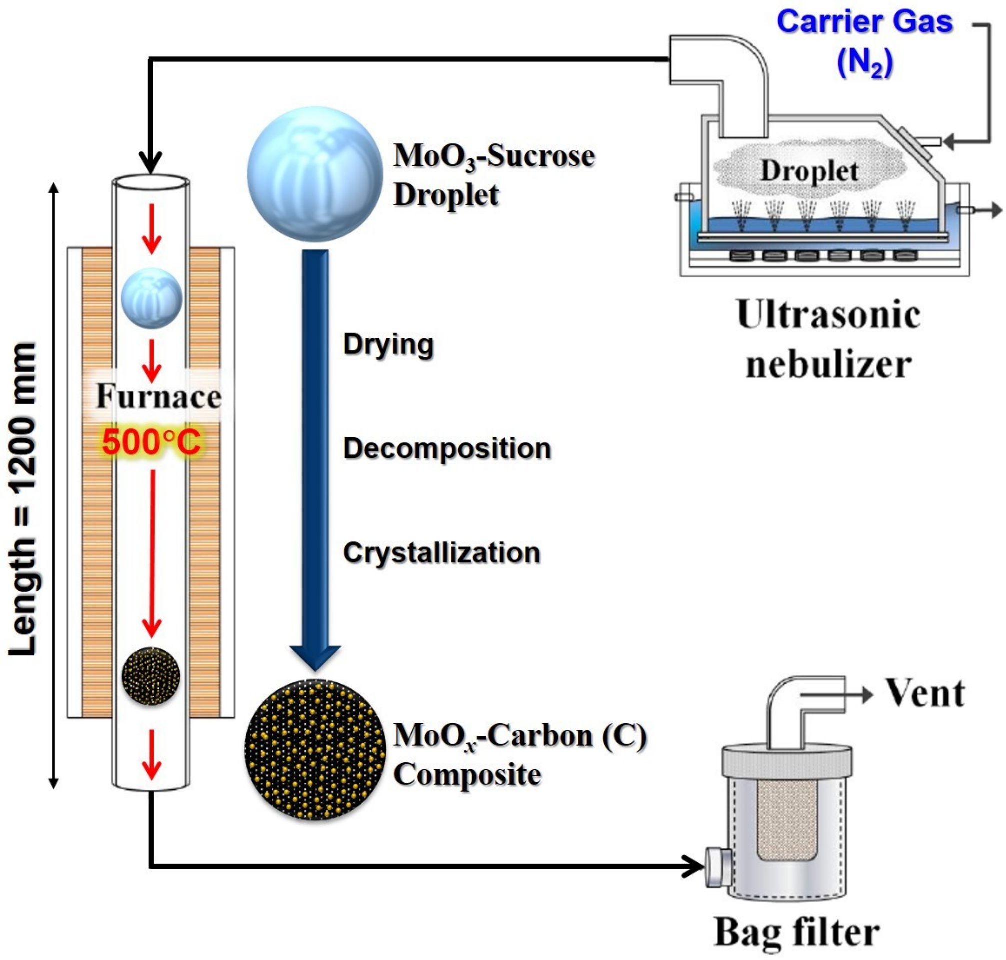

Fig. S1. Schematic diagram of the spray pyrolysis applied in the preparation of the C-MoO_x composite microspheres for $MoTe_2$-C composite microspheres as a precursor powder.

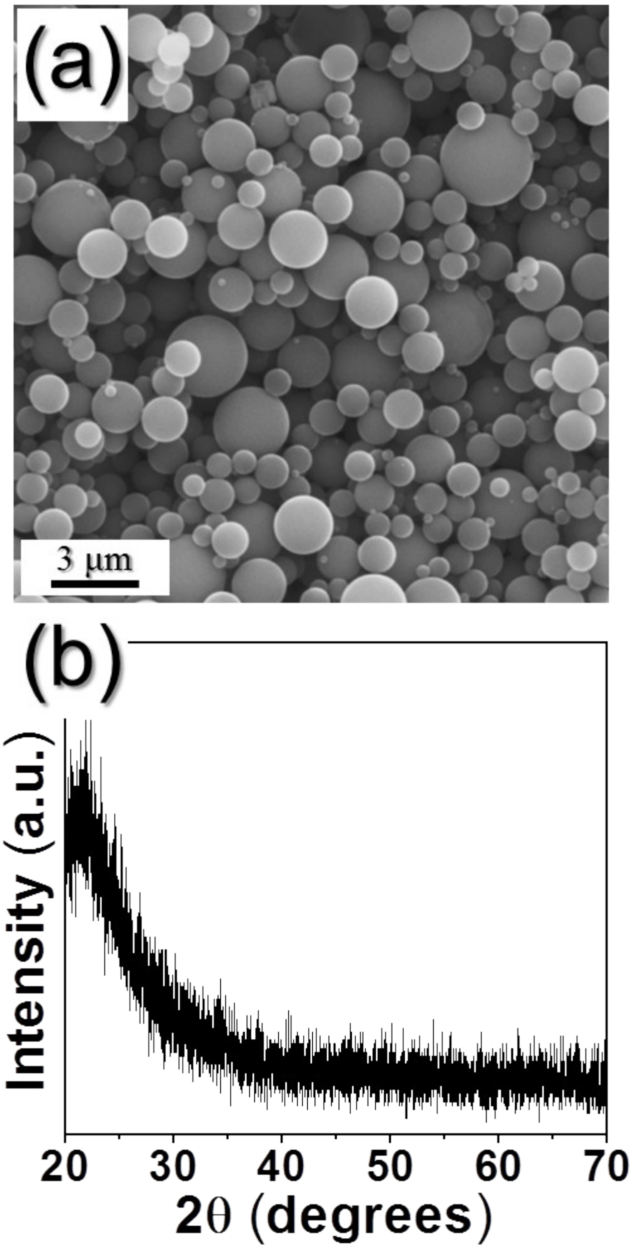

Fig. S2. Morphologies and phase analysis of the C-MoO_x composite microspheres prepared at 500 ^{o}C in N_2 atmosphere by spray pyrolysis: (a) SEM image and (b) XRD pattern.

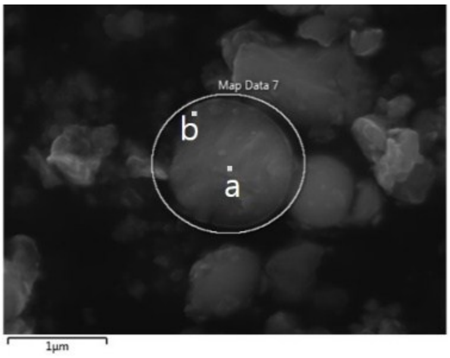

a

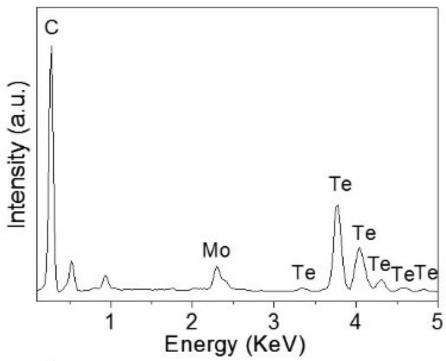

Element	Wt%
C	81.13
Mo	5.19
Te	13.78
Total:	100.00

b

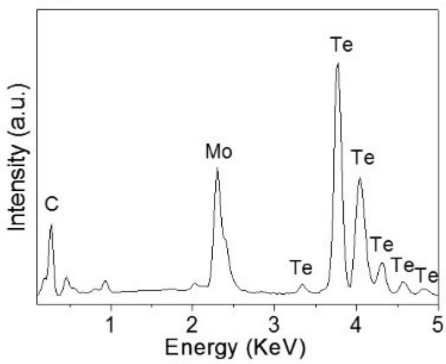

Element	Wt%
C	8.03
Mo	24.40
Te	67.57
Total:	100.00

Fig. S3. EDS analysis of the cracked C/$MoTe_2$ composite microspheres at different locations.

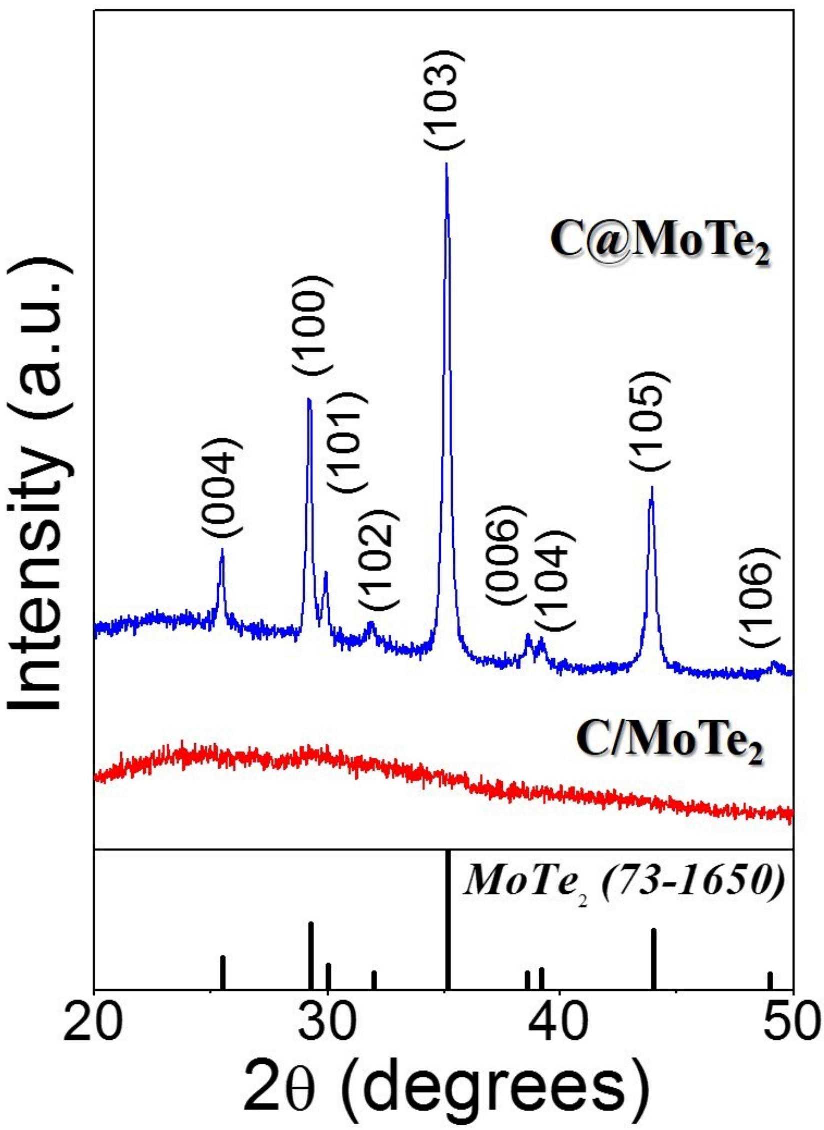

Fig. S4. XRD patterns of the core-shell-structured C@$MoTe_2$ and C/$MoTe_2$ composite microspheres formed at different tellurization temperatures.

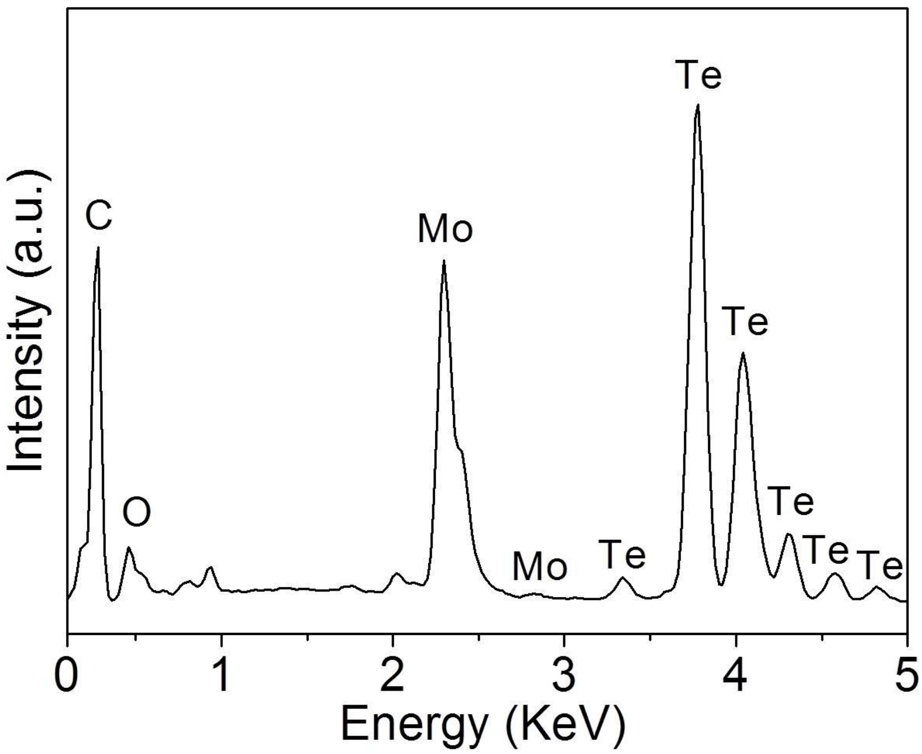

Fig. S5. EDS spectrum of the C@$MoTe_2$ composite microspheres formed by tellurization at 600 °C.

Table S1. Elemental analysis (EA) of the C@$MoTe_2$ composite microspheres formed by tellurization at 600 °C.

	C (wt %)	H (wt %)	O (wt %)	N (wt %)
C@$MoTe_2$	15.1	-	-	-

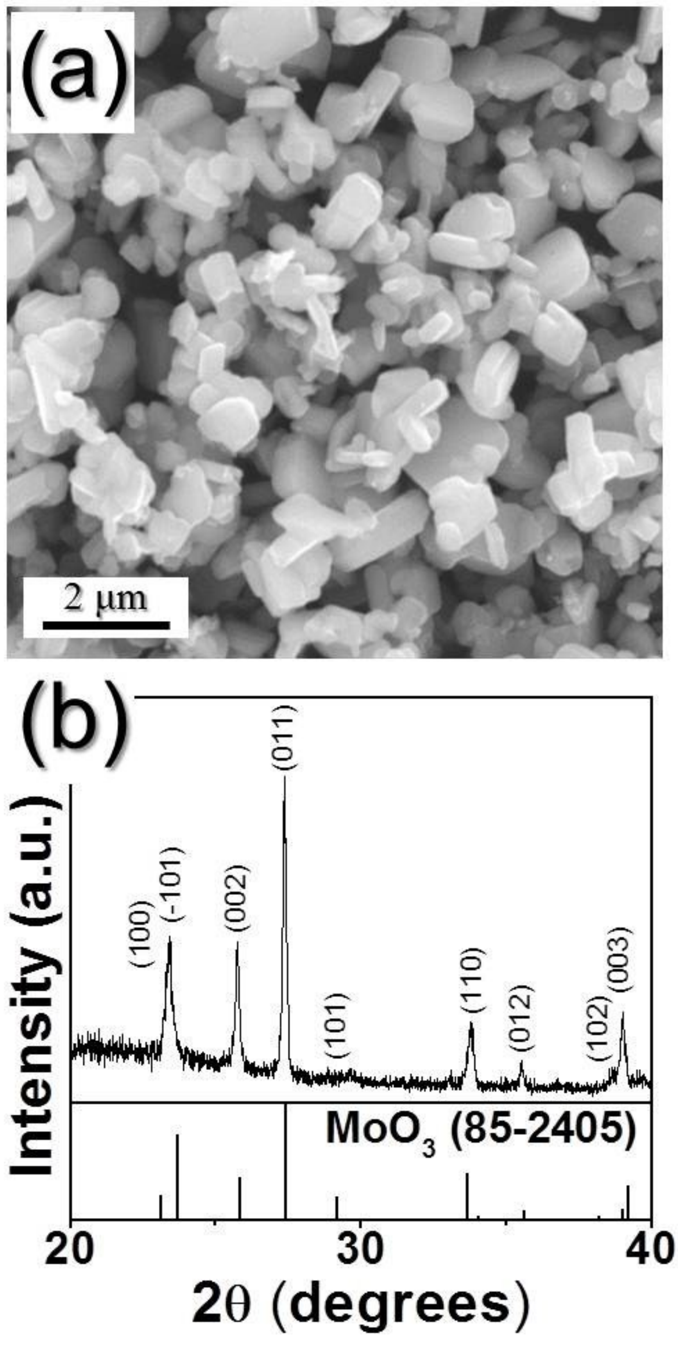

Fig. S6. SEM image and XRD pattern of the bare MoO_3 powders formed as an intermediate product for the bare $MoTe_2$ powders: (a) SEM image and (b) XRD pattern.

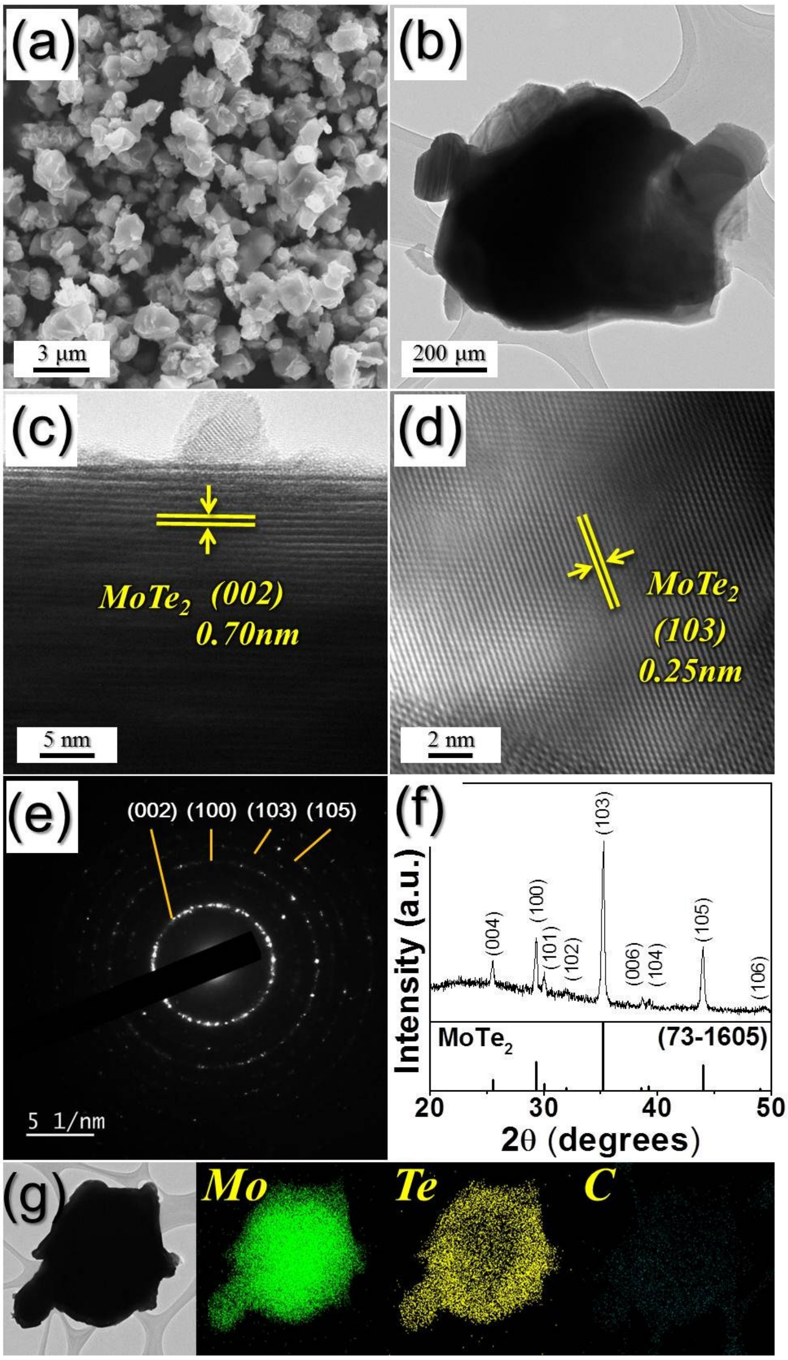

Fig. S7. Morphologies, SAED, XRD patterns, and elemental mapping images of the bare $MoTe_2$ powders as a comparison sample: (a) SEM image, (b) TEM image, (c,d) HR-TEM images, (e) SAED pattern, (f) XRD pattern, and (g) elemental mapping images.

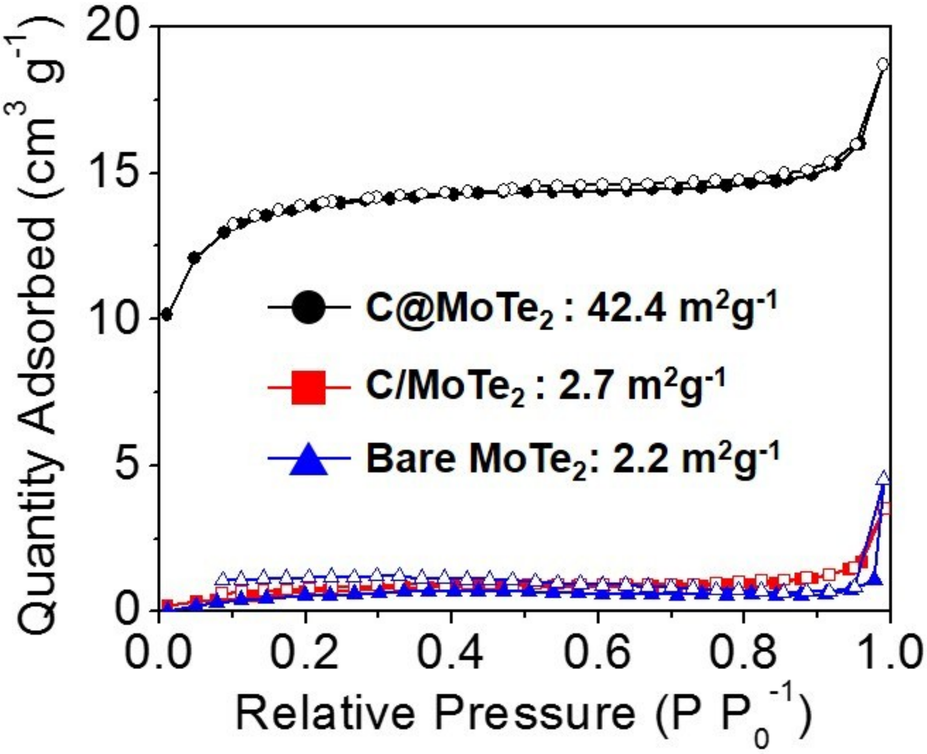

Fig. S8. N_2 gas adsorption and desorption isotherms of the core-shell-structured C@$MoTe_2$ and C/$MoTe_2$ composite microspheres and bare $MoTe_2$ powders.

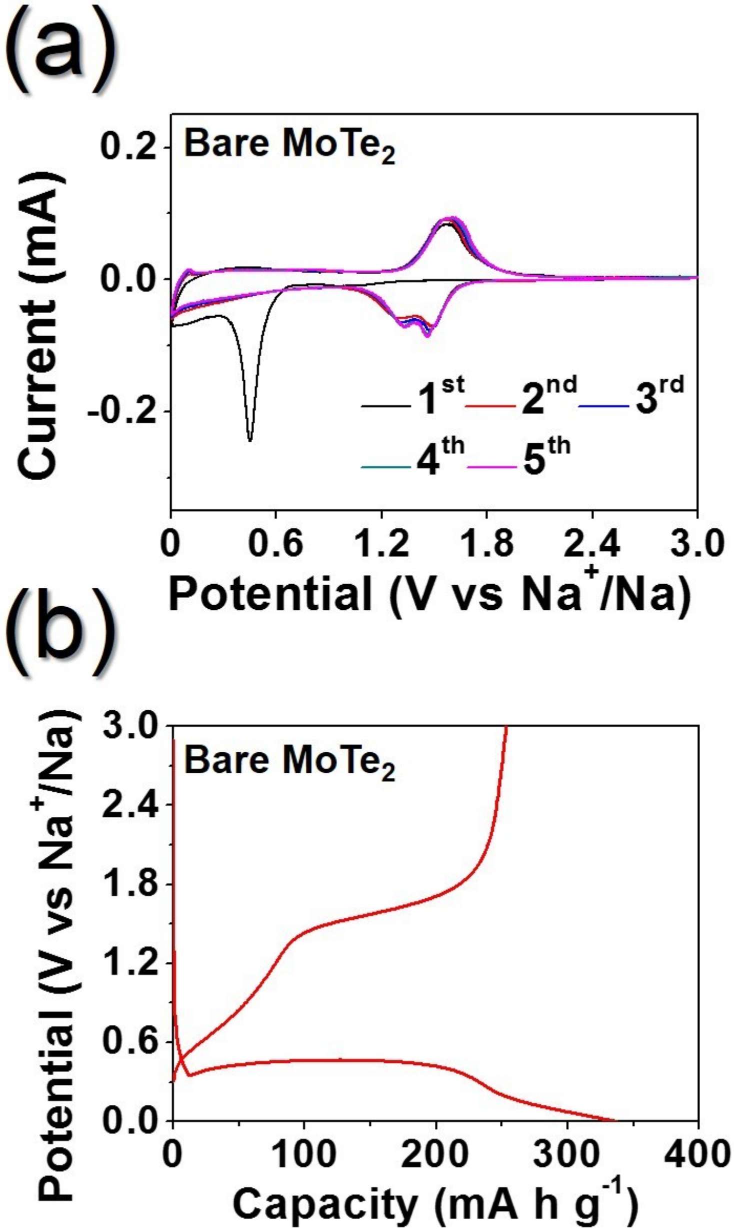

Fig. S9. (a) CV curves and (b) initial discharge-charge profiles of the bare $MoTe_2$ powders.

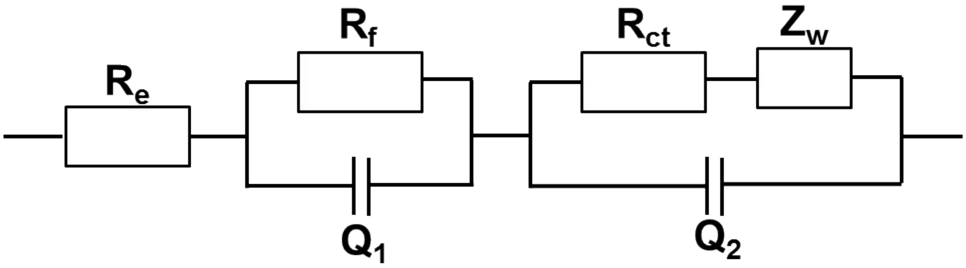

R_e : the electrolyte resistance, corresponding to the intercept of high frequency semicircle at Z_{re} axis

R_f : the SEI layer resistance corresponding to the high-frequency semicircle

Q_1 : the dielectric relaxation capacitance corresponding to the high-frequency semicircle

R_{ct}: the denote the charger transfer resistance related to the middle-frequency semicircle

Q_2 : the associated double-layer capacitance related to the middle-frequency semicircle

Z_w : the Na-ion diffusion resistance

Fig. S10. Randle-type equivalent circuit model used for AC impedance fitting.

Table S2. Sodium-ion storage properties of various transition metal dichalcogenides materials.

TMDs	Synthesis	Electrochemical properties	Ref
MoS_2/C nanospheres	Hydrothermal method	400 mA h g^{-1} after 300 cycles at 0.67 A g^{-1}	[S1]
MoS_2 nanosheet/CNTs	Hydrothermal method	495.9 mA h g^{-1} after 80 cycles at 0.2 A g^{-1}	[S2]
$MoSe_2$ yolk–shell microspheres	Spray pyrolysis	433 mA h g^{-1} after 50 cycles at 0.2 A g^{-1}	[S3]
$MoSe_2$ nanosheet/MWCNTs	Hydrothermal method	459 mA h g^{-1} after 90 cycles at 0.2 A g^{-1}	[S4]
C-$MoSe_2$/rGO	Hydrothermal method	445 mA h g^{-1} after 350 cycles at 0.2 A g^{-1}	[S5]
$NiSe_2$-rGO-C composite nanofiber	Electrospinning	468 mA h g^{-1} after 100 cycles at 0.3 A g^{-1}	[S6]
$FeSe_2$ Microspheres	Hydrothermal method	372 mA h g^{-1} after 2000 cycles at 1.0 A g^{-1}	[S7]
Urchin-like $CoSe_2$	Solvothermal method	410 mA h g^{-1} after 1800 cycles at 1.0 A g^{-1}	[S8]
Nickel disulphide graphene nanosheets composites	Hydrothermal method	407 mA h g^{-1} after 200 cycles at 0.087 A g^{-1}	[S9]
C@$MoTe_2$	Spray pyrolysis	286 mA h g^{-1} after 200 cycles at 1.0 A g^{-1}	This study

[S1] J. Wang, C. Luo, T. Gao, A. Langrock, An Advanced MoS_2/Carbon Anode for High-Performance Sodium-Ion Batteries. *Small* **11**, 473–481 (2015).

[S2] S. Zhang, X. Yu, H. Yu, Y. Chen, P. Gao, C. Li, C. Zhu, Growth of Ultrathin MoS_2 Nanosheets with Expanded Spacing of (002) Plane on Carbon Nanotubes for High-Performance Sodium-Ion Battery Anodes. *ACS Appl. Mater. Interfaces* **6**, 21880–21885 (2014).

[S3] Y. N. Ko, S. H. Choi, S. B. Park, Y. C. Kang, Hierarchical $MoSe_2$ yolk–shell microspheres with superior Na-ion storage properties. *Nanoscale* **6**, 10511–10515 (2014).

[S4] Z. Zhang, X. Yang, Y. Fu, K. Du, Ultrathin molybdenum diselenide nanosheets anchored on multi-walled carbon nanotubes as anode composites for high performance sodium-ion batteries. *J. Power Sources* **296**, 2–9 (2015).

[S5] D. Xie, W. Tang, Y. Wang, X. Xia, Y. Zhong, D. Zhou, D. Wang, X. Wang, J. Tu, Facile fabrication of integrated three-dimensional C-$MoSe_2$/reduced graphene oxide composite with enhanced performance for sodium storage. *Nano Research* **9**, 1618–1629 (2016).

[S6] J. S. Cho, S. Y. Lee, Y. C. Kang, First Introduction of $NiSe_2$ to Anode Material for Sodium-Ion Batteries: A Hybrid of Graphene-Wrapped $NiSe_2$/C Porous Nanofiber. *Sci. Rep.* **6**, 23338 (2016).

[S7] K. Zhang, Z. Hu, X. Liu, Z. Tao, J. Chen, $FeSe_2$ Microspheres as a High-Performance Anode Material for Na-Ion Batteries. *Adv. Mater.* **27**, 3305–3309 (2015).

[S8] K. Zhang, M. Park, L. Zhou, G. Lee, W. Li, Y. Kang, J. Chen, Urchin-Like $CoSe_2$ as a High-Performance Anode Material for Sodium-Ion Batteries. *Adv. Funct. Mater.* DOI:10.1002/adfm.201602608 (2016).

[S9] T. Wang, P. Hu, C. Zhang, H. Du, Z. Zhang, X. Wang, S. Chen, J. Xiong, G. Cui, Nickel Disulfide−Graphene Nanosheets Composites with Improved Electrochemical Performance for Sodium Ion Battery. *ACS Appl. Mater. Interfaces* **8**, 7811−7817 (2016).